Article ID: 1007-7294(2024)12-1891-17

Analytical Solution for Plastic Responses of Metal Beams under Repeated Impacts Based on Membrane Factor Method

GUO Kai-ling[1,2], *ZHANG Yi-jiang*[2], *MU Meng-ying*[2], *ZHU Ling*[2]

(1. Key Laboratory of High Performance Ship Technology (Wuhan University of Technology), Ministry of Education, Wuhan 430063, China; 2. School of Naval Architecture, Ocean and Energy Power Engineering, Wuhan University of Technology, Wuhan 430063, China)

Abstract: Marine structures are frequently subjected to repeated impact loadings, resulting in failure of the structures, even causing serious accidents. The analytical expressions of dimensionless permanent deflection and impact force of a metal beam based on maximal normal yield surface are derived by membrane factor method (MFM), then the results are compared with repeated impact tests. It can be found that the solutions based on MFM are between the upper and lower bounds, and very close to the results of the repeated impact tests, indicating the theoretical model proposed can predict the plastic responses of the metal beam accurately. What's more, the influences of impact location and boundary condition on the dynamic responses of the beam subjected to repeated impacts are determined. Results show that, as the distance of impact location from the middle span of the beam increases, the permanent deflection decreases, while the impact force increases. Meanwhile, the influences of impact location enhance as the impact number increases. When the permanent deflection is smaller than the thickness, the effect of boundary condition on the plastic responses is significant. However, when the deflection is larger than the thickness, the beam will be like a string and only axial force works, resulting in little influence of boundary condition on the plastic responses of the beam.

Key words: repeated impact; theoretical analysis; membrane factor method; impact location; boundary condition

CLC number: U661.4 **Document code:** A **doi:** 10.3969/j.issn.1007-7294.2024.12.007

0 Introduction

Marine structures are frequently subjected to repeated impact loadings such as collision from supplying ships, dropped objects, floe ice, etc. during navigation and operation, the damage will accumulate, leading to failure of the structures, even causing serious accidents. Therefore, it is necessary to investigate the dynamic behavior of marine structures under repeated impact loadings.

In order to determine the dynamic behavior of marine structures subjected to repeated impact

Received date: 2024-06-22

Foundation item: Supported by the National Natural Science Foundation of China (12202328; 12172265)

Biography: GUO Kai-ling(1989-), male, Ph.D., associate professor; ZHU Ling(1962-), male, Ph.D., professor, corresponding author, E-mail: lingzhu@whut.edu.cn.

loadings, investigations based on theoretical analysis, numerical simulations and impact tests were employed by many academics. Zhu[1-2] developed a numerical program based on finite difference method and conducted repeated collision tests on fully-clamped rectangular plates to analyze the dynamic responses of ship plates suffering from repeated loadings, and the expression of permanent deflection was derived. Truong et al[3-4] experimentally and numerically investigated the influences of low temperature on steel beams and grillage structures subjected to repeated lateral impacts, results show that the permanent deflections at low temperature are smaller than those at room temperature, and the effects are enlarged as the impact number increases. Zhu et al[5] performed repeated impact tests on stiffened plates, and established theoretical model based on square yield surface which can provide analytical predictions of permanent deflection. Zeng et al[6] conducted experiments on circular mild steel plates with surface cracks subjected to repeated impacts at low temperature, and the influences of low temperature as well as surface cracks on peak impact force and permanent deflection were discussed. Recently, He and Soares[7-10] experimentally and numerically studied the dynamic behavior of metal beam under repeated impacts, the characteristics of permanent deflection, contact force, and energy absorption were analyzed, and meanwhile the phenomenon of pseudo-shakedown was discussed. Cai et al[11] performed experimental and numerical studies on the dynamic behavior of steel plates suffering from repeated ice impacts, and analyzed the conditions of the occurrence of pseudo-shakedown considering the energy consumption of ice during repeated impacts.

Recently, increasing attentions have been paid to dynamic behavior of structures suffering from repeated impact loadings, and some other structures have been investigated, such as pipes and sandwich structures. Zhu et al[12] conducted repeated wedge mass impacts on tubular pipes, and the dynamic responses including impact force, deflection, and energy absorption were examined. Zhu et al[13] established numerical model on metal foam sandwich beams (MFSBs) under repeated impacts, and investigated the relationship between energy absorption of MFSBs with impact number. Guo et al[14] applied experimental studies on MFSBs subjected to repeated impact loadings, the deformation modes and failure modes of MFSBs were discussed.

To simplify the solving process in analyzing the dynamic plastic responses of structures, it is common to employ square yield surface to obtain bounds of solution[15]. However, the bounds of solution are range values, as the deflection increases, the difference between upper solution and lower solution increases, meaning the accuracy of solution becomes lower. The maximal normal stress yield surface can be also used to analyze the dynamic plastic response of structures, and its results will be much more accurate, while the control equation contains nonlinear term, resulting that it is difficult to solve the equation.

In order to obtain much more accurate solutions and reduce the difficulty in solving the equation, Membrane Factor Method (MFM) was first proposed by Yu and Strong[16] based on maximal normal stress yield criteria to study the plastic responses of beam suffering from mass impact. In this method, the effect of bending moment and axial force were both considered, and the axial force was connected with bending moment by membrane factor. Once the membrane factor was obtained, the energy consumed by bending moment and axial force could be easily given. Afterwards, the MFM

was employed to determine the dynamic plastic response of beam subjected to impulsive loadings, and the expression of dimensionless permanent deflection was derived by Yu and Chen[17]. What's more, the MFM was used to examine the dynamic behavior of beam lying on metal foam foundation, and the dimensionless deflection was adopted[18]. Subsequently, Qin and Wang[19] used MFM to investigate the dynamic plastic responses of porous metal sandwich beam suffering from blast loadings, and the accuracy of theoretical solution was verified by comparing the results with those of numerical simulations. Tian et al[20-21] expanded the application of MFM on saturated analysis of pulse loaded beams, results show that the permanent deflections obtained from MFM are more accurate than those of square yield surface.

Numerous theoretical studies have been published on the mechanical behavior of beam and plate under single impact. However, the dynamic responses of structures under repeated impacts are much different from those of single impact. When a structure suffers from repeated impact loadings, the deformation and damage of the structure will accumulate, therefore the mechanism of deformation accumulation and energy absorption cannot be revealed by simply employing the traditional method used in single impact. Meanwhile, the dynamic plastic responses of beam and plate under repeated impacts were analyzed based on square yield surface, and only the bounds of solution were obtained. By comparison, when the MFM is used in theoretical model, the interaction between bending moment and axial force can be considered. Therefore, it is crucial to use MFM to investigate the plastic mechanical behavior of structures subjected to repeated impact loadings, which can describe the mechanism of deformation accumulation, and improve the accuracy of permanent deflection prediction.

In this paper, the MFM is employed to analyze the plastic responses of metal beams under repeated impact loadings. Firstly, the theoretical model is established based on rigid plastic assumption. Subsequently, the theoretical solution is compared with result of impact tests to verify the accuracy of the theoretical model. Finally, the influences of boundary condition and impact location on the plastic responses of beams under repeated impacts are determined.

1 Fundamental theories

1.1 Geometric compatibility

In this study, the metal beam is subjected to low velocity impact with wedge mass, the sketch of which is presented in Fig.1. The length of the beam is $L_B = 2L$, the distance from the impact location to the left boundary is $L_1 = \alpha L$, and to the right is $L_2 = \beta L$. The thickness and width of the beam are H and b, respectively. V_0 is the initial impact velocity, G_s and G_B are the masses of the impactor and the beam, respectively. W is the deflection of the beam, and e and θ are the extension rate and angular rotation rate of the beam, respectively. The boundary coefficient is presented by γ, which ranges from 0 to 1. When the mass of the rigid wedge is very large relative to the beam, the stage of travelling hinge can be neglected[15]. Then, the deformation pattern of the beam subjected to impact with wedge striker can be assumed to be linear as shown in Fig.2.

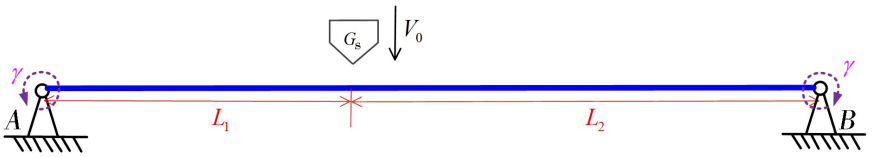

Fig.1 Sketch of the beam subjected to wedge mass impact

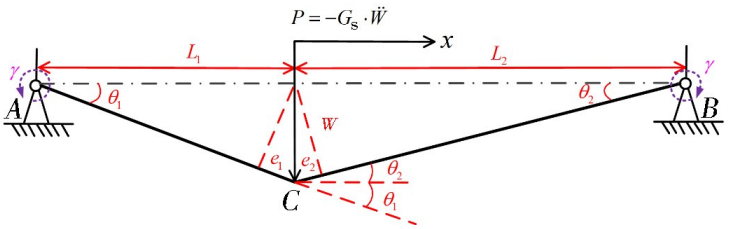

Fig.2 Deformation pattern of the beam under wedge mass impact

The total extensionof the beam is the sum of two sides, i.e.

$$e=\frac{1}{2}\left(\frac{1}{\alpha}+\frac{1}{\beta}\right)\frac{W^2}{L} \tag{1}$$

The two ends of the beam are assumed to be spring boundary, the spring coefficient is γ, then the total angular rotation can be expressed as

$$\theta_m=(1+\gamma)\left(\frac{1}{\alpha}+\frac{1}{\beta}\right)\frac{W}{L} \tag{2}$$

From Eqs.(1) and (2), the rate of extension $\dot{\varepsilon}$ and rate of angular rotation $\dot{\theta}_m$can be given

$$\dot{\varepsilon}=\dot{e}=\left(\frac{1}{\alpha}+\frac{1}{\beta}\right)\frac{W\cdot\dot{W}}{L} \tag{3}$$

$$\dot{\kappa}=\dot{\theta}_m=(1+\gamma)\left(\frac{1}{\alpha}+\frac{1}{\beta}\right)\frac{\dot{W}}{L} \tag{4}$$

Combing Eqs.(3) and (4), yields

$$\frac{\dot{\varepsilon}}{\dot{\kappa}}=\frac{W}{1+\gamma} \tag{5}$$

1.2 Flow rule

According to associated flow rule, we obtain

$$\frac{\dot{\varepsilon}}{\dot{\kappa}}=-\frac{\mathrm{d}M}{\mathrm{d}N}=-\frac{M_0}{N_0}\cdot\frac{\mathrm{d}m}{\mathrm{d}n}=2n\cdot\frac{M_0}{N_0} \tag{6}$$

$$M_0=\frac{1}{4}\sigma_Y bH^2 \tag{7}$$

$$N_0=\sigma_Y bH \tag{8}$$

where, M and N are moment and axial force of the beam, respectively, M_0 and N_0 are yield moment and yield axial force, $m=\frac{M}{M_0}$, $n=\frac{N}{N_0}$. Meanwhile, σ_Y is the yield strength of the material of the beam.

From Eqs.(6)–(8), the above equation can be simplified as

$$\frac{\dot{\varepsilon}}{\dot{\kappa}}=\frac{n}{2}H \tag{9}$$

Then, we have

$$n = \frac{2W}{(1+\gamma)H} \tag{10}$$

The state of force and moment of the beam can be seen in Fig.3.

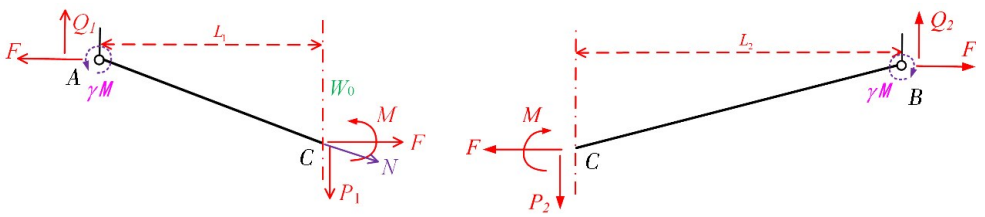

(a) Left part (b) Right part

Fig.3 Force and moments on the cross-section

The moment equilibrium equation for the beam as shown in Fig.3(a) may be written as

$$(1+\gamma)M + N \cdot W_0 + \frac{1}{3}G_B \cdot \ddot{W} \cdot L_1^2 - P_1 \cdot L_1 = 0 \tag{11}$$

Similarly, the moment equilibrium equation for the beam as shown in Fig.3(b) may be written as

$$(1+\gamma)M + N \cdot W_0 + \frac{1}{3}G_B \cdot \ddot{W} \cdot L_2^2 - P_2 \cdot L_2 = 0 \tag{12}$$

Then the inertial force of the striker can be given

$$P_1 + P_2 = P = -G_S \cdot \ddot{W} \tag{13}$$

From Eqs.(11)-(13), we can have

$$-G_S \cdot \ddot{W} = P = \frac{M_0}{L}\left(\frac{1}{\alpha}+\frac{1}{\beta}\right)\left[(1+\gamma)m + n \cdot \frac{N_0}{M_0} \cdot W_0\right] + \frac{2}{3}G_B L\ddot{W} \tag{14}$$

Defining that

$$\begin{aligned} P' &= -G_S \cdot \ddot{W} - \frac{2}{3}G_B L\ddot{W} = -G_S \cdot \ddot{W}\left(1 + \frac{2/3 \cdot G_B L}{G_S}\right) \\ &= \frac{M_0}{L}\left(\frac{1}{\alpha}+\frac{1}{\beta}\right)\left[(1+\gamma)m + n \cdot \frac{N_0}{M_0} \cdot W_0\right] \end{aligned} \tag{15}$$

The initial yield force is assumed to be $P_i = \dfrac{4M_0}{L}$, then, we can obtain

$$P^* = \frac{P'}{P_i} = \frac{1}{4}\left(\frac{1}{\alpha}+\frac{1}{\beta}\right)(1+\gamma)\left(m + n \cdot \frac{N_0}{M_0} \cdot \frac{W_0}{1+\gamma}\right) \tag{16}$$

2 Theoretical solutions

2.1 Solution based on MFM

2.1.1 Single impact

If only the plastic bending moment consumes energy, then the plastic energy absorption can be written as

$$J_m = M_0\dot{\kappa} \tag{17}$$

Therefore, when the interaction of bending moments and axial force is considered, the plastic energy absorption can be rewritten as

$$J_{mn} = M_0\dot{\kappa}\left(m + n\frac{N_0\dot{\varepsilon}}{M_0\dot{\kappa}}\right) = J_m \cdot f_n \tag{18}$$

Then the membrane force factor f_n can be defined as

$$f_n = m + n \cdot \frac{N_0}{M_0} \cdot \frac{W_0}{1+\gamma} \tag{19}$$

Combing Eq.(16) and Eq.(19), we can have

$$P^* = (1+\gamma)\left(\frac{1}{\alpha} + \frac{1}{\beta}\right) \cdot f_n \tag{20}$$

Assuming $\delta = \dfrac{W}{H}$, if $n = \dfrac{2W}{(1+\gamma)H} = 1$, then $\delta = \dfrac{W}{H} = \dfrac{1+\gamma}{2}$

(1) If $0 \leqslant \delta \leqslant \dfrac{1+\gamma}{2}$

The membrane force factor can be expressed as

$$f_n = 1 + \frac{4\delta^2}{(1+\gamma)^2} \tag{21}$$

(2) If $\delta \geqslant \dfrac{1+\gamma}{2}$, only the axial force N works, while the bending moment M=0, i.e. n=1 and m=0.

The membrane force factor can be obtained:

$$f_n = \frac{4\delta}{1+\gamma} \tag{22}$$

If only the plastic bending moment is considered, the plastic energy consumption can be expressed as

$$D_m = \int_0^{\Delta} J_m \mathrm{d}\Delta = (1+\gamma)\left(\frac{1}{\alpha} + \frac{1}{\beta}\right)\int_0^{\delta_0} \frac{M_0}{L/H}\mathrm{d}W \tag{23}$$

While, when the interaction between bending moment and axial force is considered, the plastic energy can be modified as

$$D_{mn} = (1+\gamma)\left(\frac{1}{\alpha} + \frac{1}{\beta}\right)\int_0^{\delta_0} f_n \cdot \frac{M_0}{L/H}\mathrm{d}W \tag{24}$$

(1) If $0 \leqslant \delta \leqslant \dfrac{1+\gamma}{2}$, we have

$$D_{mn} = (1+\gamma)\left(\frac{1}{\alpha} + \frac{1}{\beta}\right)\left[\delta + \frac{4}{3}\delta^3 \cdot \frac{1}{(1+\gamma)^2}\right]\frac{M_0}{L/H} \tag{25}$$

(2) If $\delta \geqslant \dfrac{1+\gamma}{2}$, we obtain

$$D_{mn} = (1+\gamma)\left(\frac{1}{\alpha} + \frac{1}{\beta}\right)\left[\frac{1+\gamma}{6} + \frac{2}{1+\gamma}\delta^2\right]\frac{M_0}{L/H} \tag{26}$$

As for the problem of large mass impact, energy consumption in the stage of travelling hinge is relatively small, indicating the initial kinetic energy of the wedge mass is mainly consumed in the stage of stationary hinge[15]. The initial impact velocity and rebound velocity are defined as V_0 and V_r, respectively. Then at the end of the impact, the kinetic energy loss can be expressed as

$$\Delta E_K = \frac{1}{2} G_S \cdot \left({V_0}^2 - {V_r}^2 \right) \tag{27}$$

According to energy conservation, the energy equilibrium equation can be written as

$$D_{mn} = \Delta E_K \tag{28}$$

The dimensionless kinetic energy loss and plastic energy consumption can be defined as

$$\Delta E_K^* = \frac{\Delta E_K}{\frac{M_0}{L/H}(1+\gamma)\left(\frac{1}{\alpha}+\frac{1}{\beta}\right)} \tag{29}$$

$$D_{mn}{}^* = \frac{D_{mn}}{\frac{M_0}{L/H}(1+\gamma)\left(\frac{1}{\alpha}+\frac{1}{\beta}\right)} \tag{30}$$

From Eqs.(25)–(30), we can have

If $0 \leqslant \delta \leqslant \frac{1+\gamma}{2}$,

$$\Delta E_K^* = \delta + \frac{4}{3}\delta^3 \cdot \frac{1}{(1+\gamma)^2} \tag{31}$$

If $\delta \geqslant \frac{1+\gamma}{2}$,

$$\Delta E_K^* = \frac{1+\gamma}{6} + \frac{2}{1+\gamma}\delta^2 \tag{32}$$

Based on Eqs.(31)–(32), the analytical expression of the permanent deflection can be obtained.

2.1.2 Repeated impact

In the repeated impacts, the initial impact energy is assumed to be identical in each impact. The impact energy accumulates during the impact, as well as the deflection of beam. Therefore, as for the *i*th impact, we can have

$$D_{mni} = \sum_1^i \Delta E_{K_i} = \sum_1^i \frac{1}{2} G_S \left(V_0^2 - V_{ir}^2 \right) \tag{33}$$

where, V_0 and V_{ir} are the initial impact velocity and rebound velocity of the wedge mass, respectively, in the *i*th impact.

If $0 \leqslant \delta \leqslant \frac{1+\gamma}{2}$,

$$\frac{\sum_1^i \frac{1}{2} G_S \left(V_0^2 - V_{ir}^2 \right)}{\frac{M_0}{L/H}(1+\gamma)\left(\frac{1}{\alpha}+\frac{1}{\beta}\right)} = \delta + \frac{4}{3}\delta^3 \cdot \frac{1}{(1+\gamma)^2} \tag{34}$$

If $\delta \geqslant \frac{1+\gamma}{2}$,

$$\frac{\sum_{1}^{i}\frac{1}{2}G_{\mathrm{S}}\left(V_{0}^{2}-V_{ir}^{2}\right)}{\frac{M_{0}}{L/H}\left(1+\gamma\right)\left(\frac{1}{\alpha}+\frac{1}{\beta}\right)}=\frac{1+\gamma}{6}+\frac{2}{1+\gamma}\delta^{2} \tag{35}$$

2.2 Bounds of the solution

When the interaction of bending moment and axial force is considered, the control equation based on circumscribing yield surface can be expressed as following:

$$-G_{\mathrm{S}}\ddot{W}_{1}\dot{W}_{1}-\int_{A}G_{\mathrm{B}}\ddot{W}\dot{W}\mathrm{d}A=\sum_{m=1}^{i}\int_{l_{m}}\left(M_{0}+N_{0}W\right)\dot{\theta}_{m}\mathrm{d}l_{m} \tag{36}$$

The force equilibrium equation for the beam as shown in Fig.3(a) may be written as

$$-G_{\mathrm{S1}}\ddot{W}_{1}\dot{W}_{1}-\int_{0}^{L_{1}}G_{\mathrm{B}}\ddot{W}_{1}\dot{W}_{1}\left(1-\frac{x}{L_{1}}\right)^{2}\mathrm{d}x=M_{0}\left[\left(1+\gamma\right)+4\frac{W_{1}}{H}\right]\frac{\dot{W}_{1}}{L_{1}} \tag{37}$$

The force equilibrium equation for the beam as shown in Fig.3(b) may be expressed as

$$-G_{\mathrm{S2}}\ddot{W}_{1}\dot{W}_{1}-\int_{0}^{L_{2}}G_{\mathrm{B}}\ddot{W}_{1}\dot{W}_{1}\left(1-\frac{x}{L_{2}}\right)^{2}\mathrm{d}x=M_{0}\left[\left(1+\gamma\right)+4\frac{W_{1}}{H}\right]\frac{\dot{W}_{1}}{L_{2}} \tag{38}$$

where the total mass is

$$G_{\mathrm{S}}=G_{\mathrm{S1}}+G_{\mathrm{S2}} \tag{39}$$

Combining Eqs.(37)−(39), we have

$$\ddot{W}_{1}+\frac{4M_{0}\left(\frac{1}{\alpha}+\frac{1}{\beta}\right)}{\left(\frac{2}{3}G_{\mathrm{B}}L+G\right)HL}W_{1}=-\frac{M_{0}\left(\frac{1}{\alpha}+\frac{1}{\beta}\right)\left(1+\gamma\right)}{\left(\frac{2}{3}G_{\mathrm{B}}L+G_{\mathrm{S}}\right)L} \tag{40}$$

To simplify the above equation, parameters h and d can be induced.

$$h=\frac{4M_{0}\left(\frac{1}{\alpha}+\frac{1}{\beta}\right)}{\left(\frac{2}{3}G_{\mathrm{B}}L+G_{\mathrm{S}}\right)HL} \tag{41}$$

$$d=-\frac{M_{0}\left(\frac{1}{\alpha}+\frac{1}{\beta}\right)\left(1+\gamma\right)}{\left(\frac{2}{3}G_{\mathrm{B}}L+G_{\mathrm{S}}\right)L} \tag{42}$$

$$\omega=\sqrt{h} \tag{43}$$

Then, Eq.(40) can be simplified as

$$\ddot{W}_{1}+hW_{1}=d \tag{44}$$

The solution to Eq.(44) obtained satisfies the following initial conditions:

$$W_{1}(0)=0 \tag{45}$$

$$\dot{W}_{1}(0)=V_{10} \tag{46}$$

The deflection and velocity are

$$W_1(t)=\frac{V_{10}}{\omega}\sin(\omega t)+\frac{d}{h}\left(1-\cos(\omega t)\right) \tag{47}$$

$$\dot{W}_1(t)=V_{10}\cos(\omega t)+\frac{d}{\omega}\sin(\omega t) \tag{48}$$

And the maximum permanent deflection is

$$W_{1\mathrm{m}}=\frac{\sqrt{d^2+hV_{10}^2}+d}{h} \tag{49}$$

Similarly, for the second impact, we have

$$W_2(t)=\frac{V_{20}}{\omega}\sin(\omega t)+\left(W_{1\mathrm{m}}-\frac{d}{h}\right)\cos(\omega t)+\frac{d}{h} \tag{50}$$

$$W_{2\mathrm{m}}=\frac{\sqrt{d^2+h\left(V_{10}^2+V_{20}^2\right)}+d}{h} \tag{51}$$

Then for the ith impact, the following can be obtained:

$$W_i(t)=\frac{V_{i0}}{\omega}\sin(\omega t)+\left(W_{(i-1)\mathrm{m}}-\frac{d}{h}\right)\cos(\omega t)+\frac{d}{h} \tag{52}$$

$$W_{i\mathrm{m}}=\frac{\sqrt{d^2+h\sum_1^i V_{i0}^2}+d}{h} \tag{53}$$

When the beam is subjected to the repeated identical impacts, we can obtain $V_{i0}=V_{10}=V_0$. When the circumscribing yield surface is used, the deflection can be expressed as

$$W_{i\mathrm{mc}}=\frac{\sqrt{d^2+ihV_0^2}+d}{h} \tag{54}$$

By comparison, when the inscribing yield surface is used, the deflection can be written as

$$W_{i\mathrm{mi}}=\frac{\sqrt{d^2+\dfrac{ihV_0^2}{0.618}}+d}{h} \tag{55}$$

If the elastic energy of the beam is considered, the rebound velocity of wedge mass should be taken into account, then Eqs.(54)–(55) can be derived as

$$W_{i\mathrm{mc}}=\frac{\sqrt{d^2+h\sum_1^i\left(V_0^2-V_{ir}^2\right)}+d}{h} \tag{56a}$$

$$W_{i\mathrm{mi}}=\frac{\sqrt{d^2+\dfrac{1}{0.618}h\sum_1^i\left(V_0^2-V_{ir}^2\right)}+d}{h} \tag{56b}$$

Then the reaction force of the beam can be expressed as

$$P'=-\left(G_{\mathrm{S}}+\frac{2}{3}G_{\mathrm{B}}L\right)\ddot{W}=\frac{M_0}{L}\left(\frac{1}{\alpha}+\frac{1}{\beta}\right)\left(1+\gamma+\frac{4W_0}{H}\right) \tag{57}$$

From Eq.(15) and Eq.(57), we can have

$$P^*=\frac{P'}{P_i}=\frac{1}{4}\left(\frac{1}{\alpha}+\frac{1}{\beta}\right)(1+\gamma)\left(1+\frac{4}{1+\gamma}\delta_0\right) \tag{58}$$

2.3 Verification for theoretical model

In naval architecture and ocean engineering, the phenomenon of structures suffering from low velocity repeated impacts with large mass is very common. To verify the accuracy of the MFM on analyzing the plastic dynamic responses of metal beams under repeated impacts with large mass, a fully-clamped beam under impact at the middle is taken as an example, and the results of MFM are compared with those of a square yield surface as well as the repeated impact tests.

The repeated impact tests on metal beam referred in this paper were conducted by drop testing machine[7]. In the repeated impact testes, as for Case MS-2, the material of the beam is mild steel. The length of beam was 250 mm, the width of the beam was 50 mm, and the thickness of the beam was 5 mm. The mass of wedge striker was 8.058 kg, and the head of the wedge had an inverted circle with a radius of 3 mm. The impact velocity was 2.97 m/s, thus the impact energy was 35.54 J. The boundary condition of the beam was fully clamped by several bolts, as shown in Fig.4.

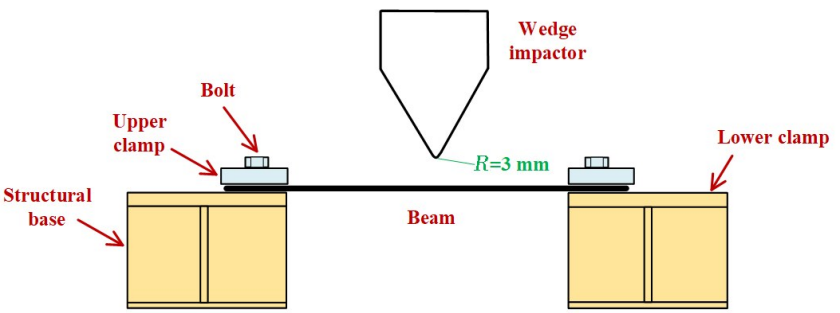

Fig.4 Experimental apparatus of repeated impact tests on steel beam

After the mass impacted on the beam, a "V" shape deformation mode could be observed, and the plastic hinges emerged at the boundaries and middle span of the beam, as presented in Fig.5. The plastic hinges appeared at both ends and the middle span of the beam, which is coincident with the assumption of deformation model in theoretical analysis.

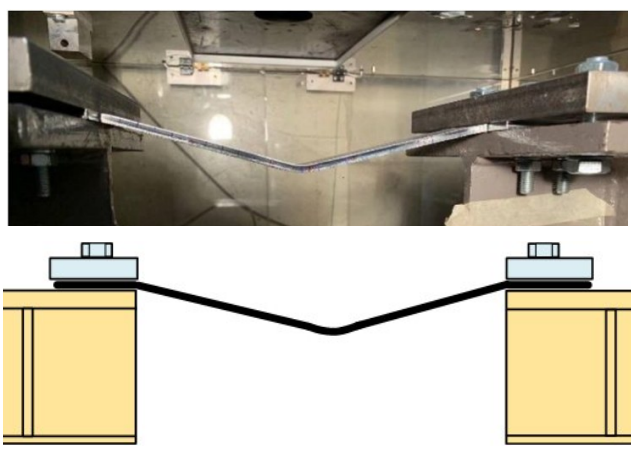

Fig.5 "V" shape deformation mode of steel beam

For the case of the impact tests, the boundary of the beam was fully clamped, and the impact location was middle of the beam. Therefore, for the theoretical model, $\gamma=1$, $\alpha=\beta=1$, then Eq.(34) and Eq.(35) can be rewritten as

$$\frac{\sum_{1}^{i}\frac{1}{2}G_{s}\left(V_{0}^{2}-V_{ir}^{2}\right)}{\frac{4M_{0}}{L/H}}=\delta+\frac{1}{3}\delta^{3} \tag{59a}$$

$$\frac{\sum_{1}^{i}\frac{1}{2}G_{s}\left(V_{0}^{2}-V_{ir}^{2}\right)}{\frac{4M_{0}}{L/H}}=\frac{1}{3}+\delta^{2} \tag{59b}$$

As for square yield surface, Eqs.(41)-(42) can be simplified as

$$h=\frac{8M_{0}}{\left(G_{S}+\frac{2}{3}G_{B}L\right)HL} \tag{60}$$

$$d=\frac{4M_{0}}{\left(G_{S}+\frac{2}{3}G_{B}L\right)L} \tag{61}$$

The initial impact energy is the kinetic energy of the striker, and after the impact, the initial impact energy is transformed into the plastic energy of the structure and rebound energy of the striker. Generally, the portion of plastic energy can be estimated simply by energy absorption ratio η_a.

It can be assumed that, after the impact, part of the initial kinetic energy of the striker has been transferred into plastic energy in form of plastic deformation, i.e.

$$\Delta E_{Ki}=\eta_{a}\cdot E_{Ki} \tag{62}$$

The beam is regarded as a rectangular beam with constant section, and it can be treated as 2D ignoring its width. In the repeated impact testes, the width of the beam is 50 mm, while in the theoretical model, the width is assumed to be the 1 mm (unit length), and therefore the correspondent impact energy of impact tests is 50 times as the theoretical model. The parameters related to the impact condition are exhibited in Tab.1, in which the unit system is used as (kg/mm/ms).

Tab.1 Parameters related to the impact condition

Parameter	Yield stress σ_Y /MPa	Length $2L$ /mm	Thickness H /mm	Beam mass G_B /kg	Bending moment M_0 /(N·m)	Axial force N_0 /kN	Striker mass G_S /kg	Impact velocity V_0/(m·s^{-1})	Kinetic energy E_K /J
Value	0.315	250	5	$3.9*10^{-5}$	1.969	1.575	0.161	2.97	0.711

From Tab.1, we have

$$\frac{G_{B}L}{G_{S}}=\frac{1}{321}\leqslant 1 \tag{63}$$

Thus, the initial force of the beam during impact can be neglected, and Eq.(15) can be modified as

$$P'=-G_{S}\cdot\ddot{W}=\frac{M_{0}}{L}\left(\frac{1}{\alpha}+\frac{1}{\beta}\right)\left[\left(1+\gamma\right)m+n\cdot\frac{N_{0}}{M_{0}}\cdot W_{0}\right] \tag{64}$$

Substituting data in Tab.1 into Eq.(34), Eq.(35) and Eq.(56), the expression of dimensionless permanent deflection W^* can be derived.

The permanent deflections predicted by theoretical model and impact tests are illustrated in

Tab.2 and Fig.6, respectively. It is obvious that, as the impact number increases, the deformation of the beam accumulates, and the permanent deflection increases, while the increment of the deflection for each impact decreases. From comparisons, we can find that the solutions based on MFM are between the upper and lower bounds based on square yield surface, and very close to the results of the repeated impact tests, indicating the theoretical model proposed in this paper are accurate to predict the plastic responses of beam subjected to repeated impacts. Meanwhile, the differences between the upper solution based on inscribing yield surface and the lower solution based on circumscribing yield surface enlarge with the increase of impact number, indicating the precision of the bounds of the solution declines as the impact energy accumulates. In addition, the deformation profiles of the beam in typical impact number (1^{st}, 5^{th}, 10^{th}) are plotted in Fig.7. It can be found that the deformation pattern of theoretical method is similar to that of the impact tests, and that the difference of permanent deflection between the theoretical method and the impact tests is very small, indicating the accuracy of the theoretical method is relatively high.

Tab.2 Permanent deflection in different impact numbers (Unit: mm)

Impact number	MFM	Circumscribing	Inscribing	Experiment
1	6.07	4.67	6.40	5.10
2	9.05	7.32	9.84	8.50
3	11.27	9.40	12.51	11.50
4	13.12	11.17	14.77	13.80
5	14.74	12.73	16.77	15.80
6	16.20	14.14	18.58	17.50
7	17.54	15.45	20.25	18.60
8	18.78	16.66	21.80	19.10
9	19.95	17.81	23.26	19.50
10	21.05	18.89	24.64	19.70

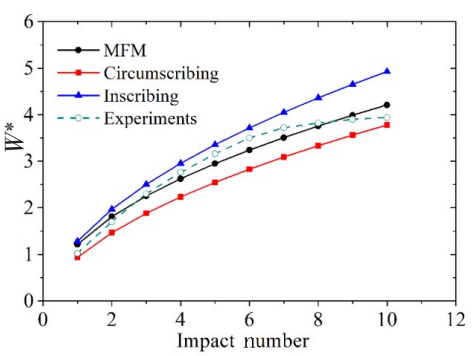

Fig.6 Correlation between dimensionless deflection with impact number

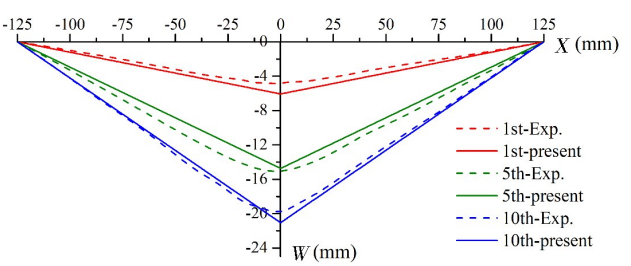

Fig.7 Comparison of deformation profiles between theoretical method and impact tests

As for the initial reaction force P_0^*, the values obtained from MFM and circumscribing yield surface are the same, while those from inscribing yield surface are 0.618 times of the MFM. As shown in Fig.8, it can be found that when the impact number is small, the results based on inscribing yield surface are much more close to those of MFM. By comparison, when the impact number is large, the results based on circumscribing yield surface are much more close to those of MFM.

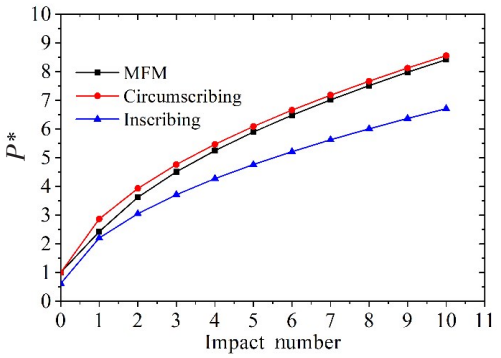

Fig.8 Correlation between force with impact number

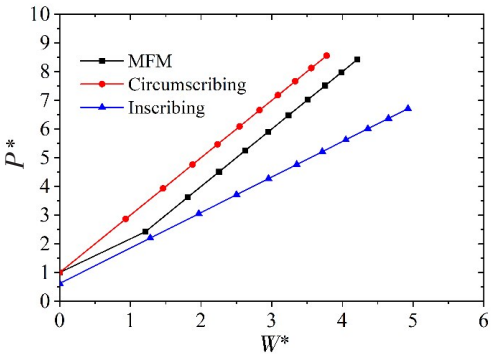

Fig.9 Correlation between force with deflection

The correlation between dimensionless force and the dimensionless deflection is plotted in Fig.9. It can be seen that when $W^*\leqslant 1$, the results obtained from circumscribing yield surface are more close to those of MFM while when $W^*\geqslant 1$, the results obtained from inscribing yield surface are more close to those of MFM.

2.4 Influence of impact location

As mentioned in Section 2.1, when the dimensionless deflection $W^*\leqslant 1$, the plastic energy consumption is decided by the axial force and the bending moment. However, when the dimensionless deflection $W^*\geqslant 1$, only the axial force works, while the bending moment is zero (M=0). For the impact tests, the dimensionless permanent deflections in the 1st impact is larger than 1. To consider the combined effect of axial force and bending moment on the plastic responses of the beam subjected to repeated impacts, in the following part, the parameters related to the impact condition are employed as listed in Tab.3.

Tab.3 Parameters related to the impact condition

Parameter	Yield stress σ_Y /MPa	Length $2L$ /mm	Thickness H /mm	Beam mass G_B /kg	Bending moment M_0 /(N·m)	Axial force N_0 /kN	Striker mass G_S /kg	Impact velocity V_0/(m·s^{-1})	Kinetic energy E_K /J
Value	0.235	50	1	7.8×10^{-6}	0.059	0.235	0.125	0.2	0.025

The stress state, geometric compatibility and deformation model significantly depend on impact location, thus different impact locations may result in different responses in form of impact force and permanent deflection. The beam with two ends fully clamped is taken as an example to discuss the influence of impact location on the dynamic plastic responses of beam under repeated impacts. In this paper, four typical impact locations are analyzed, the distances of impact location to the middle span are 0 L_s, 1/8 L_s, 1/4 L_s and 3/8 L_s, respectively, as illustrated in Fig.10.

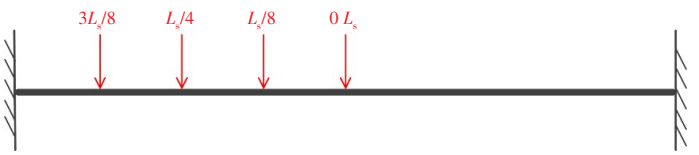

Fig.10 Sketch of impact location

From Eq.(34) and Eq.(35), we have

$$\frac{\sum_{1}^{i}\frac{1}{2}G_sV_0^2}{\frac{2M_0}{L/H}\left(\frac{1}{\alpha}+\frac{1}{\beta}\right)}=\delta+\frac{1}{3}\delta^3\quad(0\leqslant\delta\leqslant 1)\tag{65a}$$

$$\frac{\sum_{1}^{i}\frac{1}{2}G_sV_0^2}{\frac{2M_0}{L/H}\left(\frac{1}{\alpha}+\frac{1}{\beta}\right)}=\frac{1}{3}+\delta^2\quad(\delta\geqslant 1)\tag{65b}$$

Based on Eq.(16), we obtain

$$P^*=\begin{cases}\frac{1}{2}\left(\frac{1}{\alpha}+\frac{1}{\beta}\right)(1+\delta^2) & (0\leqslant\delta\leqslant 1)\\ \left(\frac{1}{\alpha}+\frac{1}{\beta}\right)\delta & (\delta\geqslant 1)\end{cases}\tag{66}$$

Substituting data in Tab.3 into Eq.(65) and Eq.(66), the dimensionless deflection and force can be obtained. The correlations of dimensionless deflection with impact number are presented in Fig.11, from which we can find the trends of curves for different impact locations are very similar, i.e. the deflection increases gradually with the increase of impact number, while the increments declines. When the impact location is at the middle span, the deflection is the largest, regardless of the impact number. By contrast, when the impact location is the farthest from the middle span, the deflection is the smallest. Opposite to the influence on deflection, the dimensionless force becomes smaller as the distance of impact location to the middle span increases, as shown in Fig.12. The influences of impact location on the plastic responses of beam enhance with the impact number.

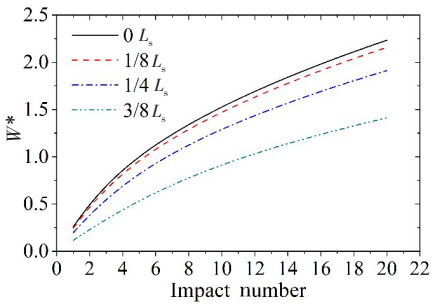

Fig.11 Dimensionless deflection in different impact numbers

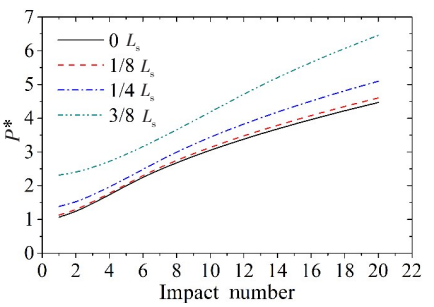

Fig.12 Dimensionless force in different impact numbers

To determine the influence of impact location on the deflection and impact force, the correlations of dimensionless deflection and force are exhibited in Fig.13 and Fig.14. It can be found that, as the distance of impact location to the middle span increases, the dimensionless deflection declines gradually, the dimensionless force increases, and the increments increase significantly.

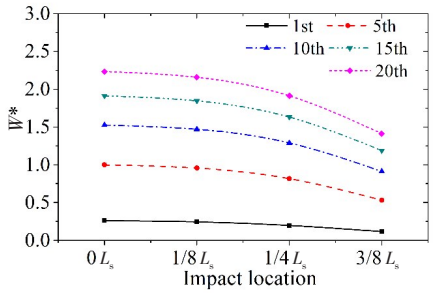

Fig.13 Dimensionless deflection at different impact locations

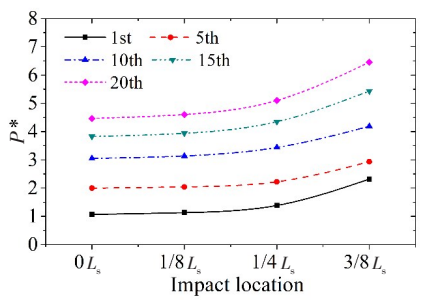

Fig.14 Dimensionless force at different impact locations

2.5 Influence of boundary condition

In reality, the boundary condition of structures is not absolutely fully clamped or simply supported, but in a state of in-between. If the boundary condition is simply supported, γ=0; while, if the boundary condition is fully clamped, γ=1. Here, the case of repeated impacts at middle span is taken as an example, in which $\alpha = \beta = 1$.

Then from Eq.(34) and Eq.(35), we have

$$\frac{\sum_1^i \frac{1}{2} G_s V_0^2}{\frac{2M_0}{L/H}(1+\gamma)} = \delta + \frac{4}{3}\delta^3 \cdot \frac{1}{(1+\gamma)^2} \qquad \left(0 \leqslant \delta \leqslant \frac{1+\gamma}{2}\right) \tag{67a}$$

$$\frac{\sum_1^i \frac{1}{2} G_s V_0^2}{\frac{2M_0}{L/H}(1+\gamma)} = \frac{1+\gamma}{6} + \frac{2}{1+\gamma}\delta^2 \qquad \left(\delta \geqslant \frac{1+\gamma}{2}\right) \tag{67b}$$

From Eq.(16), we obtain

$$P^* = \begin{cases} \frac{1}{2}(1+\gamma)\left(1 + \frac{4\delta^2}{(1+\gamma)^2}\right) & \left(0 \leqslant \delta \leqslant \frac{1+\gamma}{2}\right) \\ 2\delta & \left(\delta \geqslant \frac{1+\gamma}{2}\right) \end{cases} \tag{68}$$

The relationships of dimensionless deflection and force with impact number for different boundary conditions are illustrated in Fig.15 and Fig.16, respectively. From those figures, we can find that either for simply-supported condition or fully-clamped condition, the dimensionless deflection and force increase gradually, while the increments of them decline slowly. It can also be found that both the dimensionless deflection and force in fully-clamped condition are larger than those in simply-supported condition. Meanwhile, as the impact number increases, the influences of boundary condition on plastic responses of the beam decrease. The reason is that, when the impact number is small, the deflection is smaller than the thickness of the beam, at this moment, both the bending moment and axial force consume energy. While the impact number becomes larger, the deflection is larger than the thickness of the beam, at this moment, the beam is similar to a string, thus only the axial force works. Hence, as the impact number increases, the influence of boundary condition on the plastic responses of the beam declines.

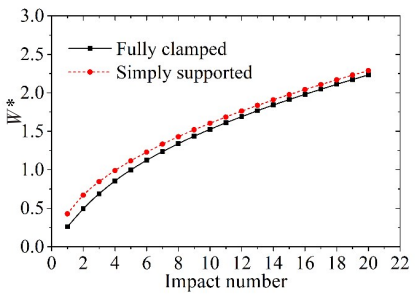

Fig.15 Effect of boundary condition on deflection

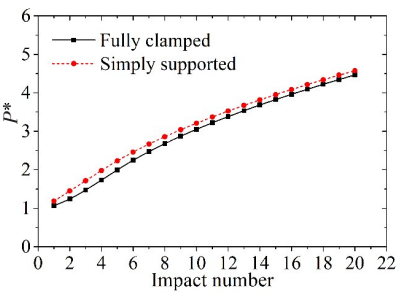

Fig.16 Effect of boundary condition on impact force

3 Conclusions

The theoretical model was established based on MFM to analyze the dynamic plastic responses of beam under repeated impact loadings. Besides, the theoretical solution was compared with the result of impact tests to verify the accuracy of the theoretical model. In addition, the influences of impact location and boundary condition on the plastic responses of beam under repeated impacts were determined. Some conclusions can be drawn as following:

(1) When a beam suffers from repeated impact loadings, the energy absorption of the beam accumulates gradually, resulting in the deflection and impact force increasing with impact number, and the increments decreasing.

(2) The deflection and impact force predicted by MFM lie between upper and lower solutions based on square yield surface, which agrees well with the results of impact tests, indicating the MFM is accurate to predict the dynamic plastic responses of beam subjected to repeated impacts. As for small deflection, solutions based on inscribing yield surface is much more accurate than those of circumscribing. By comparison, for larger deflection, the results based on circumscribing are much more accurate.

(3) The influence of impact location on the dynamic plastic responses of beam under repeated impacts is significant. As the distance from the impact location to middle span increases, the deflection increases and the impact force decreases, while the increment declines. Meanwhile, the influence of impact location enlarges with the increase of impact number.

(4) The influence of boundary condition on the dynamic plastic responses depends on the ratio of deflection to thickness. When the permanent deflection is smaller than beam thickness, the boundary condition will have significant influence on the plastic responses. By contrast, when the permanent deflection is larger than beam thickness, owing to the beam mainly suffering from axial stretch, the difference of deflection and impact force between simply-supported condition and fully-clamped condition is relatively small, indicating the influence of boundary condition is weakened.

References

[1] Zhu L. Dynamic inelastic behaviour of ship plates in collision[D]. Scotland, UK: University of Glasgow, 1990.

[2] Zhu L, Faulkner D. Damage estimate for plating of ships and platforms under repeated impacts[J]. Marine Structures, 1996, 9: 697-720.

[3] Truong D D, Jung H J, Shin H K,et al. Response of low-temperature steel beams subjected to single and repeated lateral impacts[J]. International Journal of Naval Architecture and Ocean Engineering, 2018, 10(6): 670-682.

[4] Truong D D, Shin H K, Cho S R. Repeated lateral impacts on steel grillage structures at room and sub-zero temperatures[J]. Internal Journal of Impact Engineering, 2018, 113: 40-53.

[5] Zhu L, Shi S, Jones N. Dynamic response of stiffened plates under repeated impacts[J]. Internal Journal of Impact Engineering, 2018, 117: 113-122.

[6] Zeng Y, Chen H, Yu R, et al. Experimental research on dynamic behavior of circular mild steel plates with surface cracks subjected to repeated impacts in low temperature[J]. Shock and Vibration, 2020(1):3713709.1-3713709.11.

[7] He X, Soares C G. Experimental study on the dynamic behavior of beams under repeated impacts[J]. Internal Journal of Impact Engineering, 2021, 147: 103724.

[8] He X, Soares C G. Numerical study on the pseudo-shake down of beams under repeated impacts[J]. Ocean Engineering,

2021, 242: 110137.
[9] He X, Garbatov Y, Soares C G. Analysis of pseudo-shakedown of rectangular plates under repeated impacts[J]. Ocean Engineering, 2022, 265: 112609.
[10] He X, Garbatov Y, Soares C G. Pseudo-shakedown of rectangular plates under repeated impacts[J]. Marine Structures, 2022, 85: 103258.
[11] Cai W, Zhu L, Qian X. Dynamic responses of steel plates under repeated ice impacts[J]. Internal Journal of Impact Engineering, 2022, 162: 104129.
[12] Zhu L, Wang X G, Guo K L, et al. Experimental studies on dynamic behavior of tubular pipes under repeated impacts[C]// The 30th International Ocean and Polar Engineering Conference, Shanghai, 2020.
[13] Zhu L, Guo K, Yu T X, et al. Dynamic responses of metal foam sandwich beams to repeated impacts[J]. Explosion and Shock Waves, 2021, 41: 073101.
[14] Guo K L, Mu M Y, Zhou S. Investigation on the dynamic behaviors of aluminum foam sandwich beams subjected to repeated low-velocity impacts[J]. Metals, 2023, 13: 1115.
[15] Jones N. Structural impact[M]. Cambridge University Press, 2011.
[16] Yu T X, Stronge W J. Large deflections of a rigid-plastic beam-on-foundation from impact[J]. Internal Journal of Impact Engineering, 1990, 9(1): 115-126.
[17] Yu T X, Chen F L. Analysis of large deflection dynamic response of rigid-plastic beams[J]. Journal of Engineering Mechanics, 1993, 119(6): 1293-1301.
[18] Xiang X M, Lu G X. Dynamic deflection of a beam on metal foam[J]. Key Engineering Materials, 2013, 535: 481-484.
[19] Qin Q H, Wang T J. A theoretical analysis of the dynamic response of metallic sandwich beam under impulsive loading[J]. European Journal of Mechanics, A/Solids, 2009, 28(5): 1014-1025.
[20] Tian L R, Chen F L, Zhu L, et al. Saturated analysis of pulse loaded beams based on Membrane Factor Method[J]. Internal Journal of Impact Engineering, 2019, 131: 17-26.
[21] Zhu L, Tian L R, Chen F L, et al. A new equivalent method for complex-shaped pulse loading based on saturation analysis and membrane factor method[J]. Internal Journal of Impact Engineering, 2021, 158: 104018.

基于膜力因子法的金属梁低速重复冲击塑性响应研究

郭开岭[1,2], 张义江[2], 穆梦颖[2], 朱 凌[2]
(1. 高性能船舶技术教育部重点实验室(武汉理工大学), 武汉 430063;
2. 武汉理工大学 船海与能源动力工程学院, 武汉 430063)

摘要: 船海结构经常遭受重复冲击载荷,导致结构失效破坏,甚至造成严重事故。本文基于最大应力屈服面,利用膜力因子法建立金属梁低速冲击塑性响应理论分析模型,获得无量纲最终挠度和无量纲冲击力的解析表达式,并将理论结果与实验结果进行对比。研究发现膜力因子法的求解结果与实验结果十分接近,且位于内外屈服面求解的结果之间,验证了理论方法具有较好的准确性。在此基础上,利用本文提出的理论方法研究冲击位置和边界条件对金属梁塑性动力响应的影响规律。结果表明,随着冲击位置距跨中增加,最终挠度不断减小,但冲击力峰值不断增大,且冲击位置的影响随着冲击次数的增大而增强。当最终挠度小于梁厚时,边界条件对金属梁塑性响应的影响较大;而当最终挠度大于梁厚时,金属梁将会类似于一根塑性弦,只有轴力做功,就会导致边界条件对塑性响应的影响非常小。

关键词: 重复冲击; 理论分析; 膜力因子法; 冲击位置; 边界条件
中图分类号: U661.4 **文献标识码:** A
基金项目: 国家自然科学基金资助项目(12202328; 12172265).

作者简介: 郭开岭(1989-),男,武汉理工大学船海与能源动力工程学院副教授;
张义江(2001-),男,硕士研究生;
穆梦颖(1999-),女,硕士研究生;
朱 凌(1962-),男,武汉理工大学船海与能源动力工程学院教授。